

# Suppression of Simultaneous Switching Noise in

# Power and Ground Plane Pairs

Parallel plate waveguide (PPW) noise, also known as simultaneous switching noise (SSN) or ground bounce noise (GBN) is one of the major concerns for the high-speed digital computer systems with fast edge rates, high clock frequencies, and low voltage levels.

The resonance modes between the power and ground (PWR/GND) planes excited by the SSN causes significant signal integrity (SI) problems and electromagnetic interference (EMI) issues for the high-speed circuits. Therefore the elimination of this noise is essential.

Adding decoupling capacitors to create a low impedance path between PWR/GND planes is a typical way to suppress SSN [1]. However, in general, these capacitors are not effective at frequencies higher than 600 MHz due to their finite lead inductance. The embedded capacitance with a very thin dielectric is another possible solution to suppress SSN; nevertheless the electromagnetic waves still propagate between the planes with resonance at specific frequencies.

A hybrid method which is considered to be an alternative to the use of decoupling capacitors is represented by virtual island (or gapped planes) and shorting vias [2]. The shorting vias are used to provide the return current path with low impedance and the virtual islands are used to block the PPW noise propagation through PWR/GND plane pairs; even with this methodology the noise suppression is only possible for very narrow band frequency ranges.

Recently, a new idea for eliminating the SSN is proposed by designing electromagnetic bandgap (EBG) structures [3-6]. When inserting an EBG structure in the parallel-plate waveguide-like structure of the power distribution network (PDN) of a printed circuit board (PCB), a resonant circuit composed of the top plate, a single patch, the corresponding via and the plane that connects the vias together is created. This circuit provides a low-impedance path to high-frequency currents in the PWR planes, suppressing propagation within specific frequency ranges.

In the present article, different configurations will be described consisting of three dimensional (3D) EBG model or more economic and alternative two dimensional (2D) planar EBG structures. The SSN noise suppression is demonstrated by means of full-wave numerical simulations based on the finite integration technique (FIT) [7]. The numerical code is validated by comparing the results due to two different solvers (time domain and frequency domain) as well as measured data.

### EBG Structures: Background

EBG structures, introduced as high-impedance surfaces (HIS) in early stages of research in this field, belong to a broad family of engineered materials called meta-materials, which have been initially employed for antenna applications because of their unique behavior.

In fact, HIS structures can satisfy a perfect magnetic conductor (PMC) condition over a certain frequency band and impose a zero degree reflection phase to normal incident waves, making them suitable for applications such as coupling reduction between antennas and antenna directivity improvement.

Although EBG HIS structures have been extensively studied, these studies have focused on open structures (not enclosed in environments like PCBs) and normal incident waves, such as antenna application; therefore, derived theories and models are only applicable to such cases. The use of EBG structures in PCB environments was first reported in [8], to suppress SSN in PCBs.

The diagram of Figure 1 illustrates the generation of SSN, the propagation of waves in the PDN, their suppression using EBG structures and their radiation from the sides of the PCB.

In summary, each row of EBG introduces transfer zeros and, at the resonance frequencies of these transfer zeros, a low-impedance path is created between the plates of the power bus, shorting all the signals propagating at that frequency.

When other rows of EBG ribbons are added to the PDN, they shift the resonance frequency of the single row ribbon, creating multiple transfer zeros, therefore a band-stop region. The overall effect of this design is therefore to shield the power bus of the PCB within a range of frequencies.

### Design of EBG Structures

There are a few primary closed form formulas for describing properties of EBG periodic structures using lumped elements model when the structure is small enough compared to wavelength. The parallel LC resonator which acts like a band stop filter is one of them. Other models are also available in literature, but, to the best of my knowledge, there is no exact or even reasonably accurate closed formula that relates the geometrical parameters of the EBGs to the frequency of band stop. Therefore, and until a highly accurate closed form expression is developed, the effective band of an EBG structure needs to be generated directly or indirectly using numerical simulation tools.

When using numerical codes to extract the effective band of these structures, several techniques are available, but two methods are commonly used: 1) direct method and 2) indirect method. In the first one, the S-parameter between two ports placed across the EBG structures ( $S_{21}$ ) is evaluated, while in

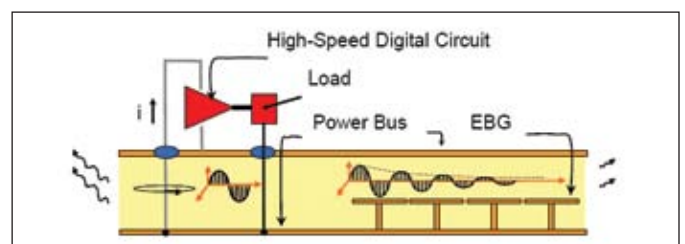


Figure 1: EBG structures embedded in PCBs: switching noise generation, radiated emissions and suppression mechanisms

the second one the so-called dispersion diagram is calculated. This diagram describes the propagation characteristics of an infinitely periodic structure composed of EBG patches.

**Direct Method**

Figure 2 represents the top view and the stack up of a standard PCB with EBG structure consisting on squared patches. The outline of entire structure is 80 by 80 mm and the EBG patch layer has 8x8 square patches. The other parameters are:  $H_1=0.25$  mm,  $H_2=1$  mm,  $d=1$ mm and  $l=9$ mm. The behavior of the structure is probed at three ports, Port 1, Port 2, and Port 3, as illustrated in Figure 2. For comparison, a solid plane pair with the same dimensions but without the EBG patch layer is studied as well.

The simulated and measured transmission coefficients are also shown in Figure 2, as well as the comparison between the

time domain (TD) and the frequency domain (FD) simulated results.

The band gap region is well defined in both simulation and measured data and a good agreement is observed over the entire frequency range.

**Indirect Method**

The indirect method consists of the evaluation of dispersion diagrams which represent propagating modes and band gaps that can potentially exist between such modes. This kind of analysis can be performed by means of eigenmode solver and periodic boundary conditions with phase shift (scan angle) parameterized. Figure 3 illustrates a typical unit cell and the settings used for the boundary conditions in the full wave simulation.

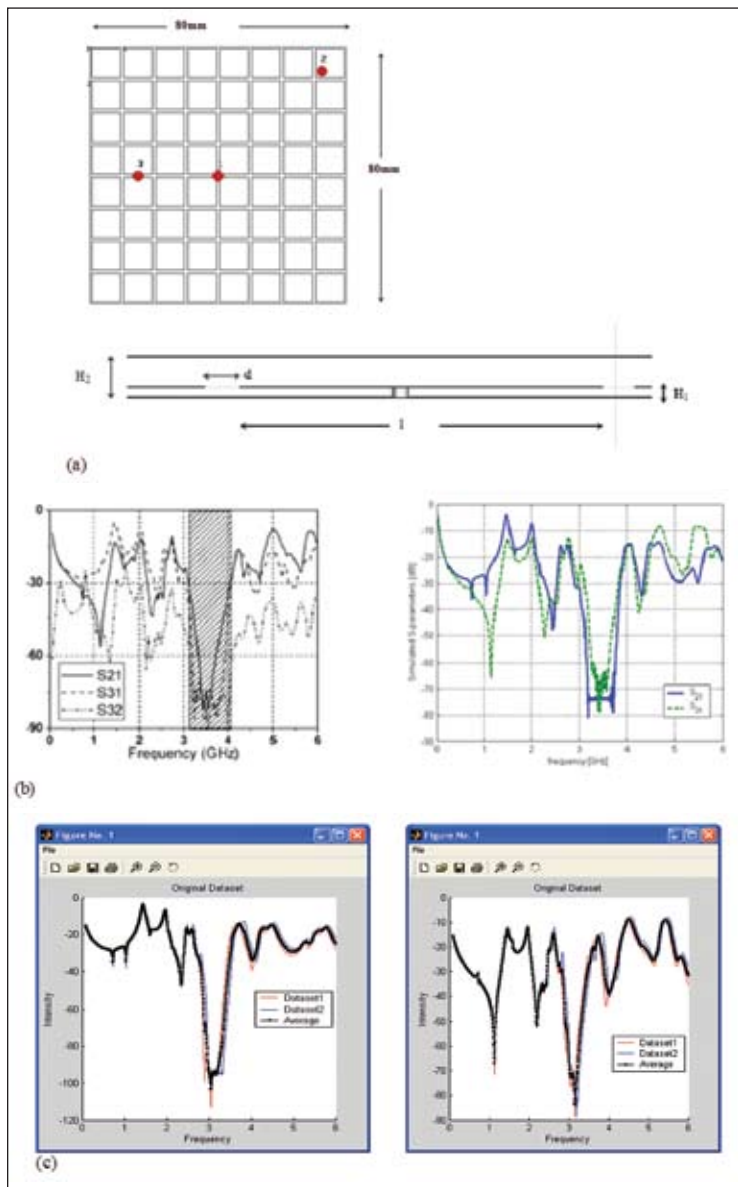


Figure 2: a) EBG structure: top view and stack-up; b)  $S_{21}$  comparison between time domain (TD) results and measured results; c) comparison between TD (Dataset1) and frequency domain (FD) (Dataset2) results

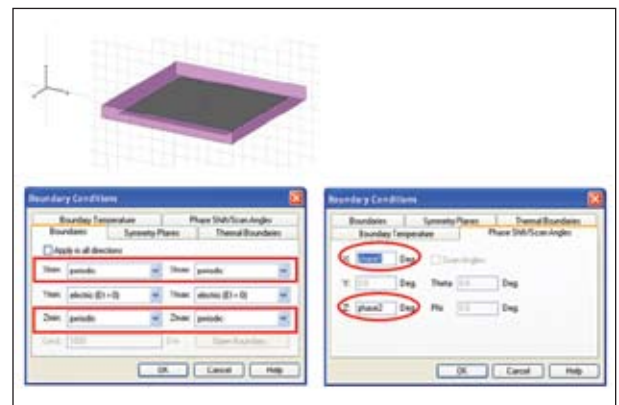


Figure 3: Unit cell and periodic boundary conditions definition

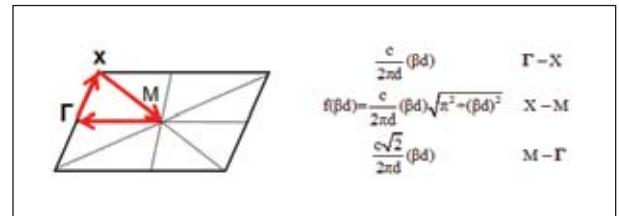


Figure 4: Brillouin triangle

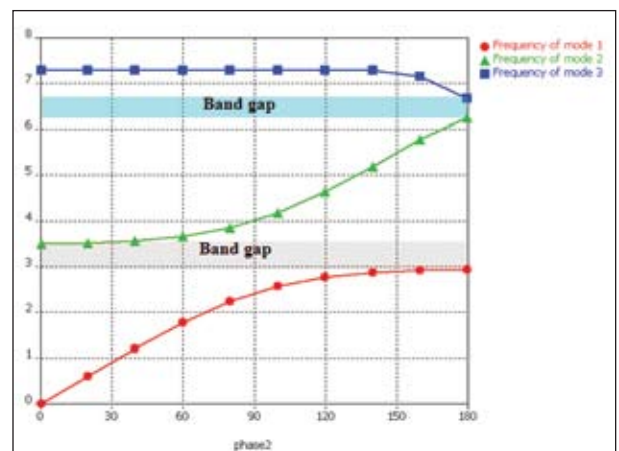


Figure 5: Dispersion diagram derived for the EBG structure illustrated in Figure 3

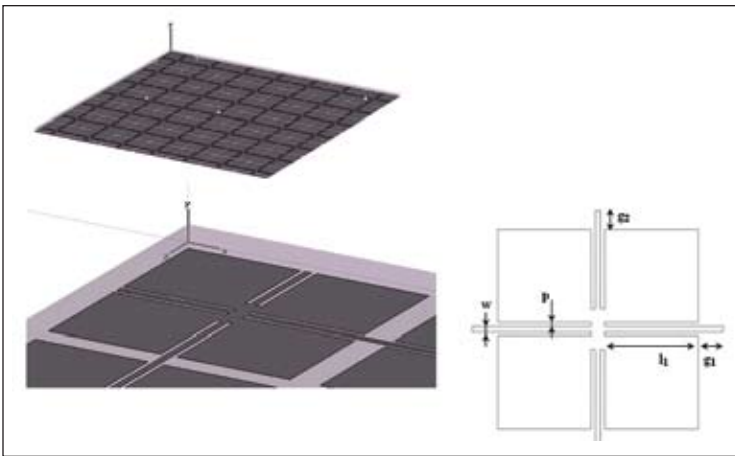


Figure 6: Schematic diagram of the proposed test board

According to the Brillouin theory, for each periodic structure there are certain vectors that constitute a boundary region of propagation. Calculating propagation modes in the direction of these vectors is sufficient to cover all the possible directions of propagation within the unit cell.

Graphically, this region is represented by the portion  $\Gamma X M$  (see Figure 4), and the equations reported in the next figure represent the frequency phase relationship, with  $d$  as the period of the structure, and  $c$  as the speed of the light in the dielectric.

A gap between the upper limit of one propagating mode and the intersection of the free space propagation line with the next propagating mode represents a region in which the surfaces do not support any propagation.

Figure 5 shows a typical dispersion diagram related to the unit cell represented in Figure 3 and obtained by varying the phase 2 between 00 and 1800 while keeping phase 1 constant. It is straightforward to evaluate the dispersion diagrams for the other directions of the Brillouin triangle.

### Two Dimensional (2D) Planar EBGs

One of the main concerns of using EBG structures for

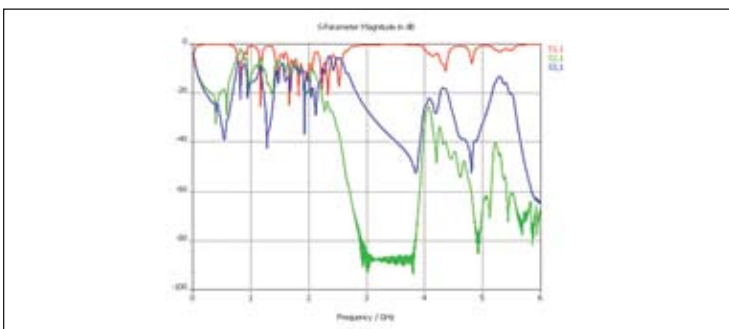


Figure 7: S-parameters of the EBG structure

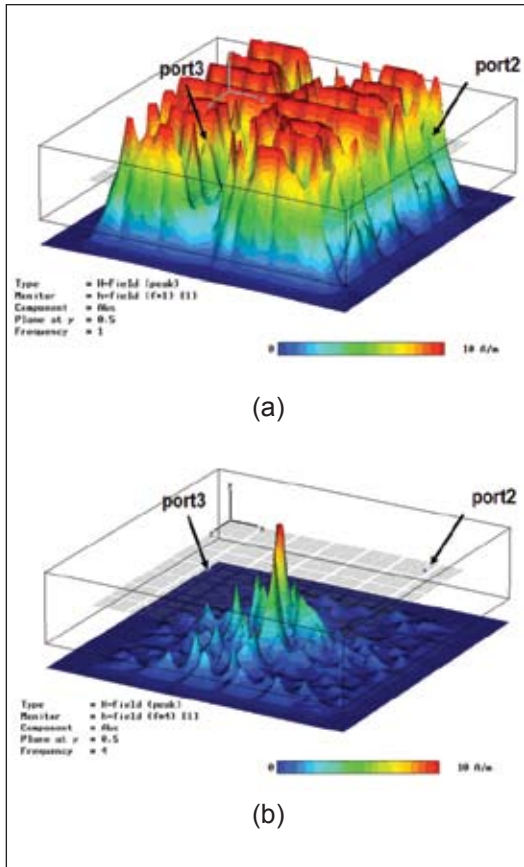


Figure 8: Magnetic field at a): 1GHz and at b): 4 GHz for the board with planar EBG structure

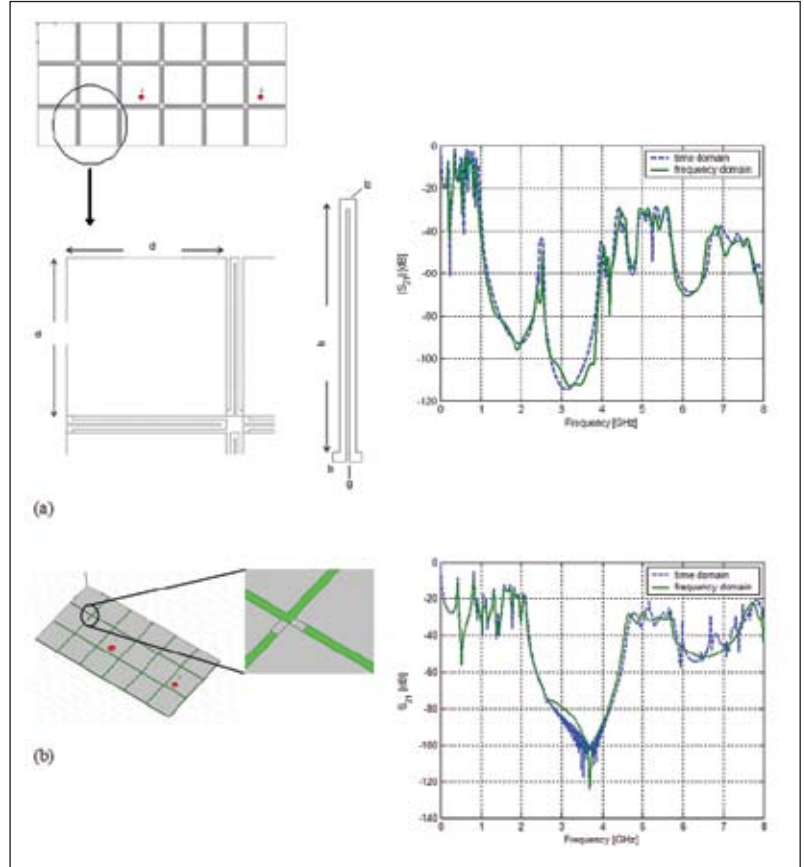


Figure 9: 2D alternative EBG structures, S21: comparison between time domain (TD) and frequency domain (FD)

SSN noise suppression is related to their cost, which can be very high. For this reason during the last few years 2D EBG structures have been proposed and extensively used for ultra wide band (UWB) noise mitigation and mixed-signal systems [9-10].

For example, a 2D EBG model is applied to the board illustrated in Figure 2; the same stack-up and the same port location are kept. In the proposed design (shown in Figure 6), the ground plane is kept continuous and 2D periodic EBG structure is designed on the power plane. The corresponding geometrical parameters of the unit cell are denoted as ( $\mathbf{a}$ ,  $\mathbf{g}_1$ ,  $\mathbf{g}_2$ ,  $\mathbf{l}_1$ ,  $\mathbf{w}$ ,  $\mathbf{p}$ ), where  $\mathbf{a}$  is the unit cell period,  $\mathbf{l}_1+\mathbf{g}_1$  and  $\mathbf{l}_1+\mathbf{g}_2$  are the bridge length in x and z directions,  $\mathbf{w}$  is the bridge width,

EBG dimensions	P	w	$l_1$	$g_1$	$g_2$	a
	0.216mm	0.288mm	5.04mm	1.36mm	1.04mm	10.8mm

**Table 1: EBG patch geometric dimensions**

parameters	d	$l_1$	$l_2$	$l_3$	g
[cm]	1.4	1.35	0.085	0.095	0.055

**Table 2: EBG Cell Dimensions**

and  $\mathbf{p}$  is the gap between the metal pad and the bridge. The dimensions of the overall parameter are listed in Table 1.

Figure 7 depicts the S-parameters of the proposed test board with EBG cells, and two clear band gaps of -40dB attenuation are observed for  $S_{21}$  over the considered frequency range: 1) 2.5-4GHz and 2) 4.2-6GHz.

The magnetic field of the proposed EBG is evaluated at two different frequencies, 1GHz (see Figure 8a), which is outside the stop band region and where we observe almost no attenuation on port 2 and port 3, and 4GHz (see Figure 8b), which is within the stop band region.

In this case, the magnetic field remains concentrated in the center of the EBG layer and the EM wave is attenuated within few patches.

Figure 9a represents another test board used to analyze the performance of the two different EBG structures. It is a 9.15x4.15cm board with FR4 dielectric ( $\epsilon_r=4.4$  and  $\tan\delta=0.02$  at 0.5GHz). The EBG layer is characterized by square patches with edge  $d=1.4\text{mm}$  and double L branches; the

# Keep Your Design ON TARGET



parameters are listed in Table 2.

Figure 9b illustrates another possible design of the metal patches (as proposed in [9-10]) for the same test board, consisting of two connected metal branches.

In the same figures the  $S_{21}$  is calculated by means of time domain and frequency domain solver, and good agreement is observed over the entire frequency range.

Figure 10 illustrates the surface current distribution at different frequencies for the board with continuous PWR plane, and the board with EBG structure (Figure 9a).

The current variation is represented by a color contrast in these figures and the color bars in which the unit is located [A]. Isolation is, of course, desirable between the two ports 2 in this example. Figure 10a shows that the EBG structure does not provide good isolation at 500 MHz, since this frequency is still in the pass band region. Figure 10b shows the current distribution on the EBG structure at 3.5 GHz, which is a frequency value in the stop band region.

The noise generated by the current source on the input port cannot propagate to the other metal patches characterizing the EBG structure, which means that eventual noise generated by

digital circuits can not propagate to the RF circuits located at the output port (port 2). It should be also noted that the scale for the surface current distribution in Figures 10a and 10b is reduced to 0-10 [A/m] in order to better visualize the surface current pattern around the input port.

### Impact of EBG Structure on the SI

Although the proposed EBG coplanar PWR/GND plane design shows excellent performance on eliminating SSN noise at broad band frequency ranges, the power planes etched slots would degrade the signal quality for the signal traces referring to the imperfect power plane. This section will discuss the impact of the proposed EBG structure on the SI.

The configuration proposed in Figure 6a is considered for this analysis, and Figure 11 shows a single-ended trace passing from the top (first) layer to the bottom layer (fourth), with two via transition along the signal path. Eye diagrams for the reference board (with continuous plane) and the EBG model are numerically evaluated.

The simulation is performed by using a mixed circuit level simulator [7] (Design Studio from CST). Two parameters, maximum eye opening (MEO) and maximum eye width (MEW) are used as metrics of the eye pattern quality.

## The Broadest Range of EMI Filter Solutions will optimize your design & lower total cost

Understanding how and where potential EMI problems exist within your system can be a major challenge. Uncovering the best way to address both conducted and radiated EMI can reduce your costs and keep your project on budget/schedule. Our experienced engineering and test team can help you find the ideal solution to satisfy global EMC standards, while meeting your design parameters.

- **Most Complete EMI Line** – We offer the flexibility to filter EMI at the power source, at the I/O connection, in a barrier wall or on the PCB. Our industry-leading line includes inductors, glass and resin seal filters, SMT filters, filter plates, filtered connectors, power entry and power line filters, and military/aerospace multisection filters.
- **MIL Qualified Products** – We offer over 800 standard QPL products & DSCC part numbers. Look to us for the largest number of MIL-PRF-15733, MIL-PRF-28861, DSCC 84084 and M11015 filters. Whether a COTS buy or engineered solution, we're the ideal source for your design.
- **EMI Design & Testing Support** – Integral to solving EMC problems is the ability to test for compliance. We conduct a wide range of EMC and environmental tests and use that data in our design process. The result is most comprehensive EMI evaluation and design resource available.
- **Meet Vendor Reduction Goals** – The breadth of products within the EMI Filter & Components Group alone can help you reduce your sourcing base. Combined with our sister divisions of Microwave, Power Management, and Sensors & Controls, you've got a real opportunity to reduce suppliers and lower overall costs.



Download our NEW  
Filter design guide on  
circular filtered connectors  
@ [www.specemc.com/guide](http://www.specemc.com/guide)

See how we can help keep your  
design on target—call

**888.267.1195**  
or visit us online.



**SPECTRUM CONTROL INC.**  
[www.specemc.com/target](http://www.specemc.com/target)

ISO 9001 QS 9000

The simulation results in MEO=0.73V and MEW=0.29ns for the reference board, and MEO=0.72V and MEW=0.27ns for the EBG board. It is interesting to note that MEO and MEW are practically the same for both models, which means no signal quality degradation.

Nevertheless an impedance variation of about 5 ohm can be observed in the TDR evaluated for the model with EBG structure if compared with the case of continuous plane, and smaller oscillations around 50 ohms are also present, probably due to the periodic gaps among the patches of the EBG cell.

In order to minimize this problem, different simulations are performed and the TDR results are reported in Figure 14. In particular, the following cases are investigated: 1) additional reference plane to provide a better return path to the current; 2) increasing the dielectric thickness on the bottom layer; and 3) changing the distance between the EBG plane and the signal traces.

As we see (Figures 14a and 14b), options 1) and 2) give consistent benefits, and the maximum deviation of the TDR

impedance is considerable reduced.

### Conclusions

The present study introduces the concept of using EBG structures for parallel plate waveguide (PPW) noise suppression. Simulated/measured results prove the effectiveness and the flexibility of this method in a range of frequencies over which the conventional methods are not effective (0.5GHz and up). The trade-off of the improved performance provided by the EBG structures is the addition of an extra metal layer.

Nevertheless, it is also demonstrated how 2D coplanar models of EBG structures allow the achievement of the same (or better) performance if compared to the more expensive 3D EBGs, while keeping a good signal quality. This is demonstrated by the calculated eye diagrams and TDR of a single-ended transmission line connecting top and bottom signal layers. A small impedance variation is observed in the TDR waveform, but possible solutions to the problem are also demonstrated. □

*A. Ciccomancini Scogna is with CST of America, Inc., and can be reached at antonio.ciccomancini@cst.com.*

### References

1. W. Cui, J. Fan, Y. Ren, H. Shi, J. Drewniak and R. DuBroof, "DC power-bus noise isolation with power plane segmentation," in *IEEE Trans. Electromagnetic Compat.*, vol.45, pag. 436-443, May 2003.
2. S. Nam, Y. Kim, H. Jang, J. Jeong at Al., "Performance analysis of signal vias using virtual island with shorting vias in multilayer PCBs," in *IEEE Trans. on Microwave Theory and Technique*, April 2005.

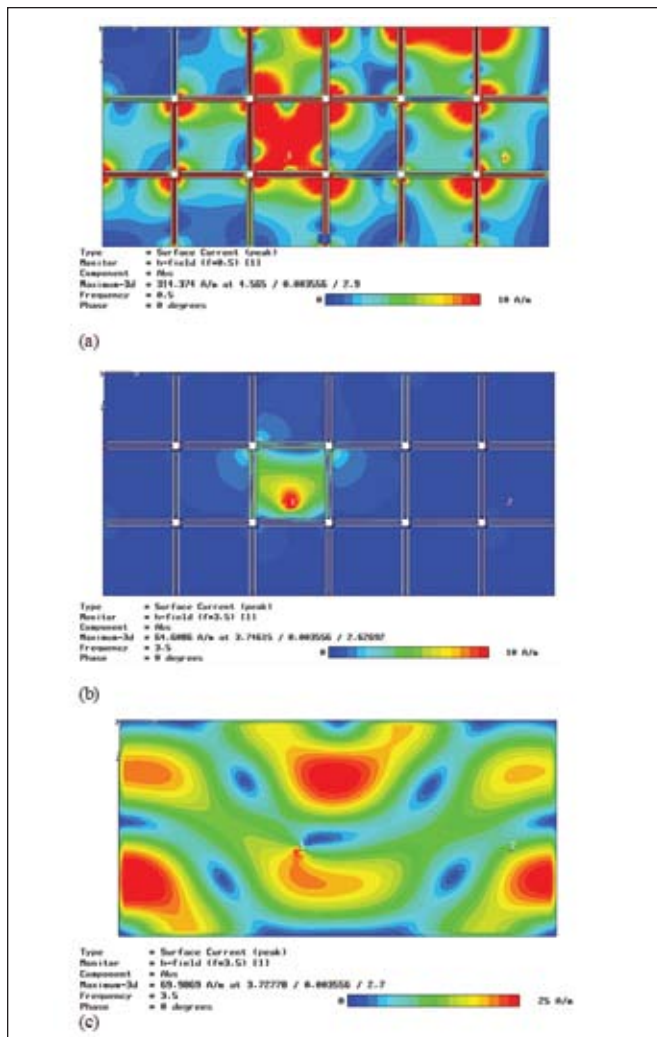


Figure 10: Surface current distribution at (a): 0.5GHz on EBG plane, (b): 3.5GHz on EBG plane and (c) 3.5GHz on continuous reference plane

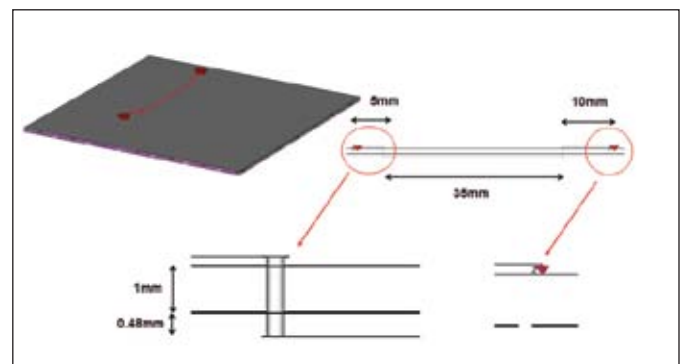


Figure 11: Single-ended transmission line and stack-up considering the board with the EBG structure of Figure 6

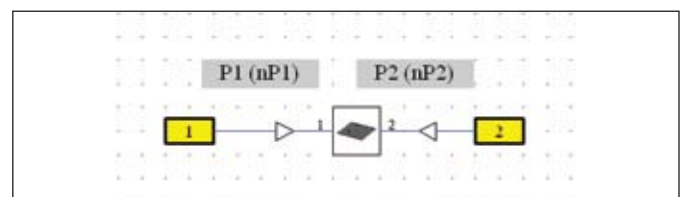


Figure 12: Design Studio model for eye diagram calculation

3. R. Abhari, G.V. Eleftheriades, "Metallo - dielectric electromagnetic band gap structures for suppression and isolation of parallel-plate noise in high speed circuits," *IEEE Trans.*

*On Microwave Theory and Tech*, vol. 51, no. 6, pp. 1629–1639, June 2003.

4. S. Shahparnia, O. M. Ramahi, "Electromagnetic interference (EMI) and reduction from printed circuit boards (PCB) using electromagnetic bandgap structures," *IEEE Trans. Electromagnetic Comp*, vol. 46, no. 4, pp. 580–587, November 2004.

5. S. Shahparnia, O. M. Ramahi, "A simple and effective model for electromagnetic bandgap structures embedded in printed circuit boards," *IEEE Microwave and Wireless Comp. Letters*, vol. 15, no. 10, pp. 621–623, October 2005.

6. A. Ciccomancini Scogna, M.Schauer, "A Novel Electromagnetic Bandgap Structure for SSN Suppression in PWR/GND plane pairs," *IEEE Proceeding of ECTC*, May 2007, Nevada, USA.

7. CST StudioSuite2006 B, also available at [www.cst.com](http://www.cst.com).

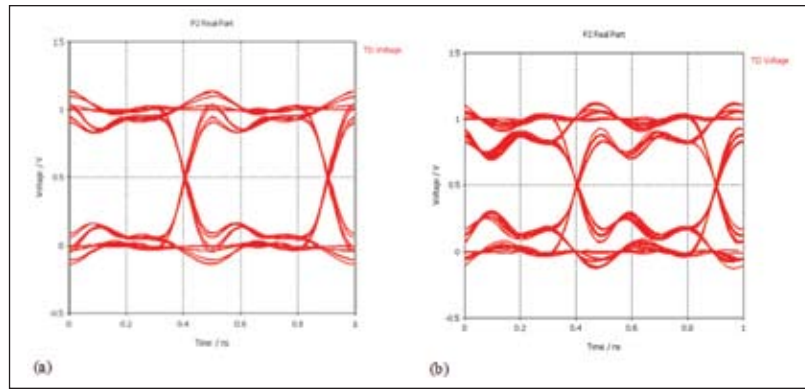


**Figure 13: Simulated eye diagram, (a) Reference board (continuous power plane) with single-end trace, (b) EBG structure**

8. S. Shahparnia, O. M. Ramahi, "Electromagnetic interference (EMI) and reduction from printed circuit boards (PCB) using electromagnetic bandgap structures," *IEEE Trans. Electromagnetic Comp*, vol. 46, no. 4, pp. 580–587, November 2004.

9. J. Choi, V. Govind, M. Swaminathan, "A novel electromagnetic band gap (EBG) structure for mixed signal system applications," Proc. of *IEEE Radio and Wireless*, Atlanta, Georgia, September 2004.

10. J. Choi, V. Govind, M. Swaminathan et al., Noise suppression and isolation in mixed signal systems using alternative impedance electromagnetic bandgap (AI-EBG) structure," accepted for *IEEE Trans. on Electromagnetic Compatibility*.

**FAST Link** [www.conformity.com/0660](http://www.conformity.com/0660)

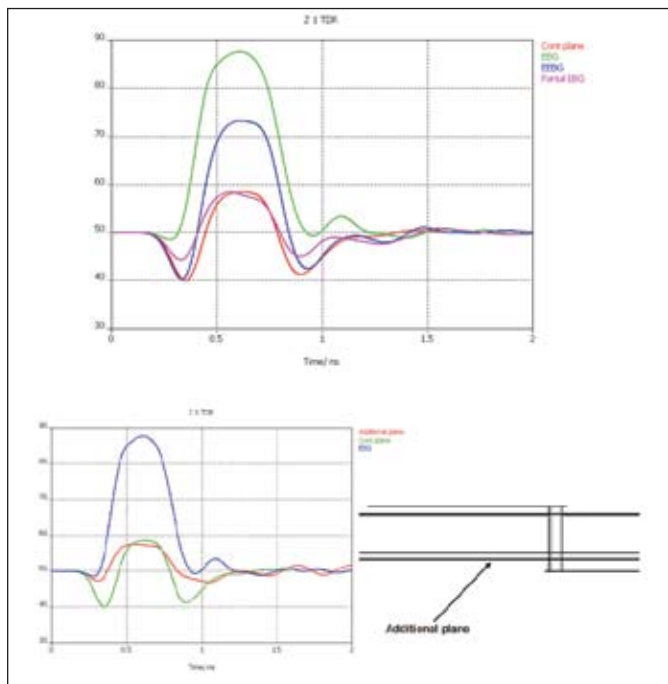


**Figure 14: TDR waveform for different configurations**

## High Current Surface Mount EMI Filters

- Models SSM (up to 10 Amps) & PSM (up to 20 Amps)
- High temperature construction
- Capacitance values to 4,000 pF (SSM) & 10,000 pF (PSM)
- Square geometry ideal for soldering to PCB
- Pi and Ft circuit available (PSM) Pi circuit (SSM)



**Visit us online or call 888.267.1195**




Ask for a **FREE** EMC Test Lab consultation @ [www.specemc.com/test](http://www.specemc.com/test)

**SPECTRUM CONTROL INC.**  
[www.specemc.com/hcsmrt](http://www.specemc.com/hcsmrt)  
**ISO 9001 QS 9000**